Satellite Potential in an Ionized Atmosphere

NORMAN C. JEN*
City University of New York, New York, N. Y.

A self-consistent field theory involving the Vlasov equation and the Poisson equation is applied to the study of the potential field around a spherical satellite, the Coulomb drag, and its wake trails in an ionized atmosphere. It is considered that undisturbed particles have a Maxwellian distribution of speeds with large mean free paths in comparison with the Debye length. In the vicinity of the sphere, both the incident and the reflected distribution functions are considered. It is found that the electrical potential around a rapidly moving satellite is not in the form of spherical symmetry, which is a new and essential contribution to the existing state of knowledge on this subject. From this nonspherical potential field, the Coulomb drag is easily formulated, and the characteristics of the wakes behind the satellite are readily predicted. The theoretical value as computed for Explorer VIII satellite leads to a potential of −0.156 v, which is in close agreement with the actual observed measurement of −0.15 v. This analysis also presents a method of obtaining results from the nonlinear and self-consistent set of Vlasov-Poisson equations.

Introduction

THE problem considered in this investigation is that of determining the potential field around a spherical satellite traveling at a constant speed in an ionized atmosphere. At the altitude of 500–1000 km, the satellite speed is several times the mean thermal speed of the atmospheric ions and many times smaller than the mean thermal speed of the electrons. Because of this, differences in charge density and in ion flux between the front and the rear of the satellite should be expected. As a consequence, the usual assumption of spherical symmetry of the potential field around a rapidly moving satellite becomes no longer valid, and a new investigation of the potential field around the satellite becomes necessary. It should be pointed out that the determination of the potential is of paramount importance since the satellite drag is directly derived from the potential. The purpose of this paper is to show a method for determining the nonspherical potential field around a spherical satellite by using the Vlasov-Poisson self-consistent field equations. It is also intended to show that the Coulomb drag and the satellite wake characteristics are closely associated with this nonspherical field. In the problem discussed in this paper, the distribution of ionized particles around the satellite is considered to be the main cause for the formation of the potential field. Such factors as the photoelectric effect and the earth's magnetic field are neglected.

In this paper, the kinetic temperatures for electrons and ions are considered to be equal or comparable. In the presence of electrons and ions of equal temperature and different masses, the satellite must receive a larger electron flux than ion flux before a negative potential field is established. The intensity of this negative potential field drops significantly to a negligible value within a distance of several Debye lengths in a manner of plasma sheath. Outside of the sheath, the potential is then assumed to be zero. In the undisturbed state, the speeds of charged particles, electrons, and ions are assumed to be in Maxwellian distribution and their mean free paths are large as compared with the Debye length. This consideration implies that the collision effect for a charged particle is small during its passage through the thin sheath, since the time interval between collisions is much larger than the time interval for the particle to pass through the sheath. This consideration does not necessarily imply that those particles are collisionless in the ionized atmosphere. The diameter of the satellite is considered to be rather large in comparison with the Debye length or the thickness of the sheath. For instance, the Debye length at the altitude of interest is in the order of centimeters, and the diameter of a satellite is in the order of meters. This consideration justifies the use of a plane-configuration approach. This analysis then involves only one space coordinate r but still retains the three velocity components of the particle.

Received February 4, 1964; revision received December 14, 1964. Part of this work was presented at the November, 1963 American Physical Society Fluid Dynamics Meeting, Massachusetts Institute of Technology, Cambridge, Mass. This work was supported by the National Science Foundation under Grant G-24490.

* Professor, School of Engineering. Member AIAA.

Two Stream Functions and Potential Profile

A set of moving coordinates is chosen such that its origin coincides with the center of the sphere and the z axis is parallel to the direction of satellite motion. Referring to this set of coordinates, the ionized gas can be treated as impinging upon a stationary sphere with normal and tangential velocity components, as shown in Fig. 1.

The undisturbed velocity distribution function of these charged particles in an elementary volume outside of the sheath region can be written as

$$f_i = \alpha \exp\{-\beta^2[(v_1 W \cos\theta)^2 + (v_2 + W \sin\theta)^2 + v_3^2]\} \quad (1)$$

where α and β are the constants; and W, the relative velocity between the satellite and the ionized gas stream. The elementary volume is located between r, θ, ϕ and $r + dr$,

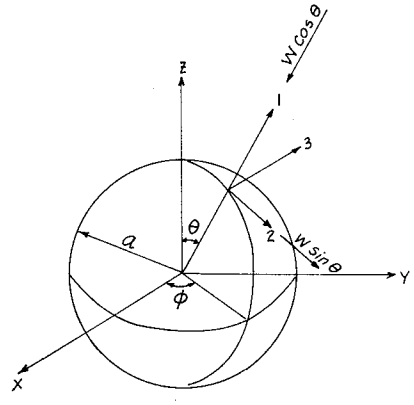

Fig. 1 Spherical satellite and its coordinates.

$\theta + d\theta$, $\phi + d\phi$. Three particular velocity components v_1, v_2, and v_3 are in the direction of r, θ, ϕ.

Within the elementary volume, the peculiar velocity component in the radial direction v_1 ranges from $+\infty$ to $-\infty$. These electrons and ions can be classified into three groups in accordance with the value of this velocity component. The first group is between $+\infty$ and $+|W\cos\theta|$, the second one is between $+|W\cos\theta|$ and $-(2q\psi_0/m)^{1/2}$, and the third is between $-(2q\psi_0/m)^{1/2}$ and $-\infty$. Here ψ_0 is the potential intensity on the satellite wall, q and m are the charge and the mass of an electron, and $(2q\psi_0/m)^{1/2}$ is the minimum value of the radial velocity for an electron that is required to penetrate through the potential field and reach the satellite wall. The first group of electrons moves away from the satellite, since the relative radial velocity is positive. The second group of electrons moves radially toward the satellite but is unable to reach the satellite wall. The third group of electrons penetrates through the potential field and reaches the satellite wall. Of course, the first group of electrons or ions has no contribution in the formation of the potential field around satellite. The second and third groups are represented by a distribution curve as shown in Fig. 2. Of course, ions of both the second and the third groups penetrate through the potential field with accelerations and strike the satellite wall. Those striking electrons could be neutralized with the striking ions on the surface and then be disassociated. It is also possible to have other complicated processes that are not yet well understood. However, it is necessary for such electrons and ions to be diffused out or reflected back from the satellite surface in order to maintain a constant satellite mass and a steady potential field. Provision for such reflection of charged particles against the satellite wall has been made in the work of Massey and Burhop,[1] Bird,[2] and Brundin.[3]

Referring to the moving coordinates, the sphere is treated as stationary, the kinetic energy of an electron in the second group remains unchanged after reflection. For stationary coordinates, as indicated by dotted lines in Fig. 2, the radial velocity is increased by $2W\cos\theta$ after reflection in a manner of a Fermi mechanism. An electron of third group strikes the satellite wall; then, leaves the wall after a certain process. The striking velocity and the reflecting velocity must be the same from the statistical viewpoint. Otherwise, it becomes impossible for the number density in the sheath region to be steady. The radial velocity component of an incident electron of the second group and its reflected velocity component are represented as point A and point A' in Figs. 2 and 3. The electron of the third group is also represented as point B and point B', respectively.

The motion of a striking ion (second and third groups) is similar to the motion of electrons of the third group, except for the acceleration toward the wall. In other words, all those charged particles (second and third groups) travel into or

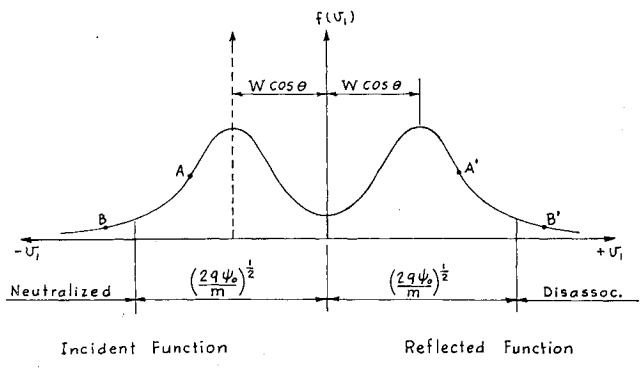

Fig. 2 Incident and reflected functions in radial direction (solid line is for moving coordinate system, and dotted line is for stationary coordinate system).

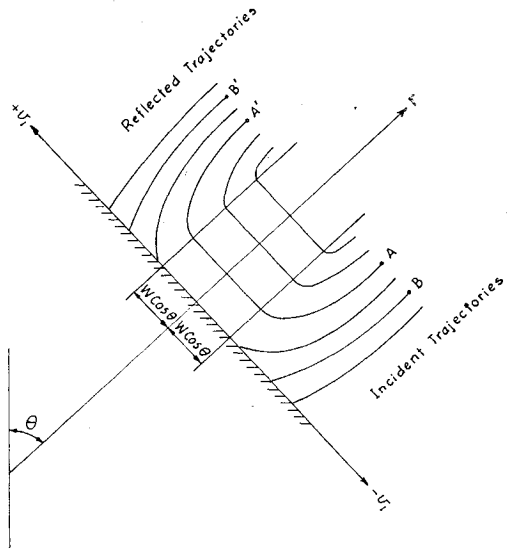

Fig. 3 Trajectories of electrons in phase space (AA' represents a typical trajectory of an electron of second group, and BB' represents a typical trajectory of an electron of third group).

through the sheath region from the field-free region; then, return into the field-free region again. The kinetic energy of each particle remains unchanged. This is equivalent to the loss of memory of each of the striking particles about its collision with the wall, while on the return trajectory, as if there were no striking or collision whatsoever. Now, the reflected function can be written as

$$f_r = \alpha \exp\{-\beta^2[(v_1 + W\cos\theta)^2 + (v_2 + W\sin\theta)^2 + v_3^2]\} \tag{2}$$

Within the sheath region, the motion of an incident electron (second or third kind) can be conveniently described by the constancy of Hamiltonian H due to the independence of time, explicitly, and its constants of canonical momenta in the 2 and 3 directions P_2 and P_5 from the geometrical symmetry:

$$\begin{aligned} H &= (1/2m)(P_1^2 + P_2^2 + P_3^2) + q\psi \\ P_1 &= m(v_1 - W\cos\theta) \\ P_2 &= mv_2 \\ P_3 &= mv_3 \end{aligned} \tag{3}$$

The foregoing equations lead to

$$(v_1 - W\cos\theta)^2 + (2q\psi/m) = \text{const} \tag{4}$$

for incidental stream function. The same leads to

$$(v_1 + W\cos\theta)^2 + (2q\psi/m) = \text{const} \tag{5}$$

for reflected stream function. The trajectory for each electron is sketched by Eqs. (4) and (5) as in Fig. 3. The substitution of the Hamiltonian into Eqs. (1) and (2) yields the following functions:

$$f_i = \alpha \exp\{-\beta^2[(v_1 - W\cos\theta)^2 + (v_2 + W\sin\theta)^2 + v_3^2 + (2q\psi/m)]\} \tag{6}$$

$$f_r = \alpha \exp\{-\beta^2[(v_1 + W\cos\theta)^2 + (v_2 + W\sin\theta)^2 + v_3^2 + (2q\psi/m)]\} \tag{7}$$

It is obvious that both distribution functions will automatically satisfy the Vlasov equation, namely,

$$\frac{\partial f}{\partial t} + \mathbf{c}\cdot\frac{\partial f}{\partial \mathbf{r}} + \mathbf{F}_e\cdot\frac{\partial f}{\partial \mathbf{c}} = 0 \tag{8}$$

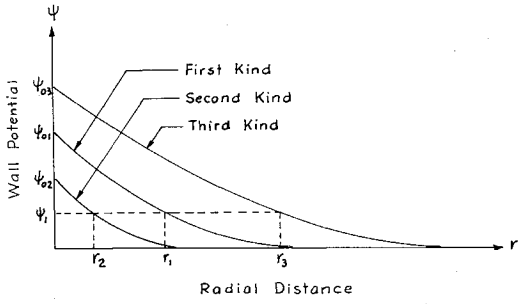

Fig. 4 Potential profiles.

where $\mathbf{c}$ is the velocity vector, $\mathbf{F}_e = (-q/m)(\partial\psi/\partial\mathbf{r})$ is the external force derived from the electric potential field. Boltzmann's H-theorem[4] has proved that the results of Eqs. (6) and (7) can be obtained by solving the Vlasov equation.

The electron density inside the sheath region due to the incident stream function can be expressed as

$$\int_{\infty-}^{+\infty}\int_{-\infty}^{+\infty}\int_{-\infty}^{2W\cos\theta} \alpha \exp\{-\beta^2[(v_1 - W\cos\theta)^2 + (v_2 + W\sin\theta)^2 + v_3^2]\}e^{-q\psi/kT}\,dv_1dv_2dv_3 \quad (9)$$

Performing the preceding integration, the following result is obtained:

$$\tfrac{1}{2}n_{0e}[1 + \operatorname{erf}(\beta_- W\cos\theta)]e^{-q\psi/kT}$$

The number of reflected electrons is equal to the number of electrons in the incident stream. Thus, the total electron density becomes

$$n_e = n_{0e}[1 + \operatorname{erf}(\beta_- W\cos\theta)]e^{-q\psi/kT} \quad (10)$$

where n_{0e} is the electron density in the undisturbed state; β_- is the constant for the electron function at constant temperature. In general, the error function in Eq. (10) is small because of the high mean thermal speed of electrons. By the similar calculation for ion density, the total number density inside the sheath region becomes

$$n_i = n_{0i}[1 + \operatorname{erf}(\beta_+ W\cos\theta)]e^{+q\psi/kT} \quad (11)$$

where n_{0i} is the ion density in the undisturbed state and β_+ is the constant for the ion function at constant temperature. Equation (11) indicates that the ion density around the satellite increases with temperature, since, under actual condition, the value of $q\psi/kT$ is relatively small and the value of n_{0i} is proportional to the temperature. Now, the Poisson equation can be written as

$$\nabla^2\psi = -(q/\epsilon)[n_e - n_i] \quad (12)$$

where ϵ is an electric constant.

Under steady-state condition, the electric current across an elementary area on the satellite surface must be zero, otherwise the potential field around the satellite can not remain steady. The condition of zero current requires that

$$n_{0i}(C_+ + W\cos\theta)e^{+q\psi_0/kT} = n_{0e}(C_- + W\cos\theta)e^{+q\psi_0/kT} \quad (13)$$

where C_- and C_+ are the mean thermal speeds of electrons and ions, and ψ_0 is the potential on the satellite wall. From Eqs. (12) and (13), the profile of the potential field is completely specified. These potential profiles can also be classified into three kinds in accordance with the value of θ. The first kind is of $\cos\theta = 0$. Equation (13) gives a wall potential ψ_{01}, and Eq. (12) becomes the ordinary plasma sheath equation. The sheath profile is well known, as shown in Fig. 4. The second kind is of $\cos\theta > 0$. Equation (13) gives a smaller wall potential ψ_{02}, and Eq. (12) gives a potential profile with larger curvature in comparison with the first kind. The third kind is of $\cos\theta < 0$. Equation (13) and Eq. (12) lead to larger potential and smaller curvature in comparison with the first kind. Three corresponding potential profiles are shown in Fig. 4. For a certain value of potential ψ_1, these potential profiles give three radii r_1, r_2, and r_3 at the three corresponding values of θ. By plotting r_1, r_2, and r_3 in Fig. 5, the equipotential surface (or line) around the satellite is obtained.

As the speed of the satellite increases to the order of several times the mean thermal speed of ions, Eq. (13) indicates that the negative potential ψ_0 becomes extremely large in the rear part of the satellite. This high potential field attracts the ion streams from its surroundings; the motion of the ion streams now becomes similar to the Rand[5] sink formulation and resembles the flow pattern of two-stream instability.[6] Such instability indicates the existence of ion oscillation with high frequency and small damping. Small damping leads to a long wake trail behind the satellite.

The difference in ion density along a diameter of the satellite is a function of the angular position and the undisturbed ion density, as indicated by Eq. (11)

$$Kn_{0i}\operatorname{erf}(\beta_+ W\cos\theta)e^{+q\psi_0/kT} \qquad 0 < \theta < (\pi/2) \quad (14)$$

where $K = 2$ for a satellite speed less than the mean thermal speed of the ions, and $K = 1$ for a satellite speed greater than the mean thermal speed. The Coulomb drag force on the satellite F due to the charged ions can be calculated by

$$F = \pi a^2 \int_0^{\pi/2} pe^{+q_0\psi/kT}\sin 2\theta d\theta \quad (15)$$

where a is the radius of the satellite, and p is the difference of pressure intensity along a diameter of the satellite. In Eq. (15), p is given as

$$p = Kn_{0i}\operatorname{erf}(\beta_+ W\cos\theta)kT \quad (16)$$

which is a known result from the kinetic theory of gases. In the foregoing calculations, the electron part is considered to be negligible.[7, 8]

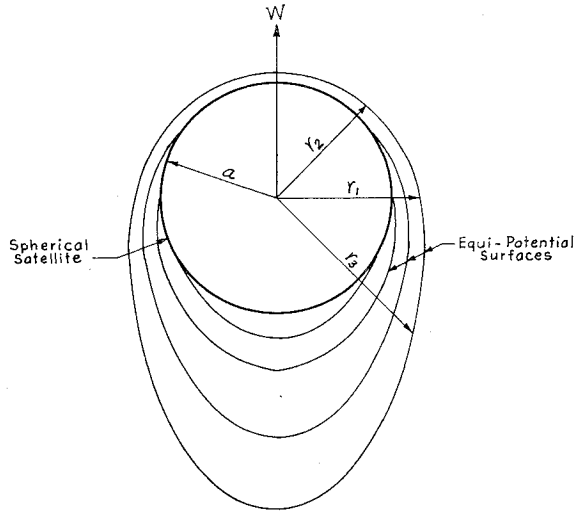

Fig. 5 Nonspherical potential field around a moving satellite (the thickness of the sheath region is enlarged).

Conclusion

Based upon the assumption of large mean free paths, the concept of incident stream function and reflected function has been developed. At the altitude of 500–1000 km, this assumption is well justified since the mean free paths are in the order of hundred meters, and the corresponding Debye

length is in the order of several centimeters. The introduction of two-stream functions makes it possible to include the satellite speed in the self-consistent equations. This analysis determines the potential field around a moving satellite, which is shown not to have spherical symmetry. Furthermore, the determined potential field is significantly associated with the calculation of Coulomb drag, as indicted in Eq. (15). Two-stream instability predicts a long wake trail behind the satellite and high frequency of oscillation which agrees with the fact. By using the actual data of Explorer VIII[9] and the data of the upper atmosphere[3] (satellite speed $= 7.4 \times 10^3$ m/sec), the mean thermal speed of electrons $= 2.06 \times 10^5$ m/sec at the altitude of 1000 km, the mean thermal speed of ions $= 1.20 \times 10^3$ m/sec, and the temperature $= 1100$ °K; Eq. (13) then gives as tagnation potential of -0.156 v as compared with the actual measurement of -0.15 v. Of course, the agreement of the surface potential with the experimental one is not a test of the potential distribution, but only of Eq. (13) and, to a lesser degree, of the assumption concerning the surface interaction. However, the interpretation[9] of Explorer VIII data supports qualitatively the nonspherical potential field.

References

[1] Massey, H. S. W. and Burhop, E. H. S., *Electronic and Ionic Impact Phenomena* (Oxford University Press, London, 1952), pp. 555–565.

[2] Bird, G. A., "The flow about a moving body in the upper ionosphere," J. Aerospace Sci. **29**, 808–814 (1960).

[3] Brundin, C. L., "Effects of charged particles on the motion of an earth satellite," AIAA J. **1**, 2529–2538 (1963).

[4] Chapman, S. and Cowling, T. G., *The Mathematical Theory of Non-Uniform Gases* (Cambridge University Press, London, 1960), pp. 69–88.

[5] Rand, S., "Wake of a satellite traversing the ionsphere," Phys. Fluids **3**, 265–273 (1960).

[6] Jackson, J. D., "Longitudinal plasma oscillations," J. Nucl. Energy: Pt. C. **1**, 171 (1960).

[7] Jastrow, R. and Pearse, C. A., "Atmospheric drag on the satellite," J. Geophys. Res. **62**, 413–423 (1957).

[8] Jen, N. C., "Plasma stress tensor on a wall," *Magnetohydrodynamics*, edited by N. Mather and G. Sutton (Gordon and Breach Scientific Publications, New York, 1962), pp. 551–558.

[9] Bordeau, R. E., Donley, J. L., Serbu, G. P., and Whipple, E. C., Jr., "Measurement of sheath currents and equilibrium potential on the Explorer VIII satellite," J. Astronaut Sci. **8**, 65–73 (1961).

APRIL 1965 AIAA JOURNAL VOL. 3, NO. 4

Optimum Estimation of Satellite Trajectories Including Random Fluctuations in Drag

H. E. RAUCH*

Lockheed Missiles and Space Company, Palo Alto, Calif.

This paper considers the problem of trajectory estimation for a low-altitude satellite when random fluctuations in atmospheric density cause noticeable changes in the motion. The standard deterministic model for satellite motion is replaced by a stochastic model; optimum estimation theory is used to obtain the best fit to the data and the model. To test the efficacy of this approach to the problem, a particular stochastic drag model and the corresponding estimation procedure have been incorporated into a computer program called "orbit fit," which is similar to one used for actual flights. The effect of drag is calculated from a standard variation of parameters with an exponential atmosphere, whereas the stochastic part of the model is based upon a first-order stationary Gauss-Markov stochastic process. Both radar data and Baker-Nunn optical data from low-altitude satellite 1960 Omicron have been run on the program, and the results are shown to be a significant improvement over those using a deterministic model, i.e., the in-track residuals are reduced from thousands of feet to hundreds of feet. In addition, the consequence of changing the correlation and variance of the stochastic model is examined. The correlation had less effect over the rms residuals than the variance. In particular, for too small a variance, the residuals reduced to those of the deterministic model, whereas for too large a variance, the residuals resulted in unstable oscillations in the estimation procedure.

I. Introduction

THE problem of estimating the trajectory of a satellite can be stated as follows: Given a series of measurements of the position of a satellite, calculate the set of parameters which specifies the path of the satellite. When air drag can be neglected, the motion of the satellite is completely determined by six parameters. These six might be the position and velocity at some initial time, or a set of six orbit elements at the time of the ascending node. From the six parameters, the current and future motion can be determined by numerical integration of the acceleration due to the earth's gravitational field or from a closed-form approximation to the integrated motion. In general, when drag is included, the assumption is usually made that its effect can also be represented as a deterministic phenomenon (for instance, as a polynomial with undetermined coefficients). This treatment may be adequate as long as drag is not a significant factor in the satellite motion. However, for many satellites, the deterministic model cannot represent the motion correctly. Fluctuations in drag (sometimes correlated with solar activity) can cause substantial

Presented as Preprint 64-396 at the 1st AIAA Annual Meeting, Washington, D. C., June 29–July 2, 1964; revision received December 18, 1964. The author wishes to express his appreciation to J. V. Breakwell for his constant encouragement and guidance during this work.

* Research Scientist, Aerospace Sciences Laboratory.